



**HAL**  
open science

## Measuring mechanical parameters in glass fiber-reinforced composites: Standard evaluation techniques enhanced by photogrammetry

Isabel Koke, Wolfgang H. Müller, Ferdinand Ferber, Rolf Mahnken, Herbert Funke

### ► To cite this version:

Isabel Koke, Wolfgang H. Müller, Ferdinand Ferber, Rolf Mahnken, Herbert Funke. Measuring mechanical parameters in glass fiber-reinforced composites: Standard evaluation techniques enhanced by photogrammetry. *Composites Science and Technology*, 2008, 68 (5), pp.1156. 10.1016/j.compscitech.2007.08.026 . hal-00498995

**HAL Id: hal-00498995**

**<https://hal.science/hal-00498995>**

Submitted on 9 Jul 2010

**HAL** is a multi-disciplinary open access archive for the deposit and dissemination of scientific research documents, whether they are published or not. The documents may come from teaching and research institutions in France or abroad, or from public or private research centers.

L'archive ouverte pluridisciplinaire **HAL**, est destinée au dépôt et à la diffusion de documents scientifiques de niveau recherche, publiés ou non, émanant des établissements d'enseignement et de recherche français ou étrangers, des laboratoires publics ou privés.

## Accepted Manuscript

Measuring mechanical parameters in glass fiber-reinforced composites: Standard evaluation techniques enhanced by photogrammetry

Isabel Koke, Wolfgang H. Müller, Ferdinand Ferber, Rolf Mahnken, Herbert Funke

PII: S0266-3538(07)00303-X  
DOI: [10.1016/j.compscitech.2007.08.026](https://doi.org/10.1016/j.compscitech.2007.08.026)  
Reference: CSTE 3794

To appear in: *Composites Science and Technology*

Received Date: 30 May 2007  
Revised Date: 24 July 2007  
Accepted Date: 9 August 2007

Please cite this article as: Koke, I., Müller, W.H., Ferber, F., Mahnken, R., Funke, H., Measuring mechanical parameters in glass fiber-reinforced composites: Standard evaluation techniques enhanced by photogrammetry, *Composites Science and Technology* (2007), doi: [10.1016/j.compscitech.2007.08.026](https://doi.org/10.1016/j.compscitech.2007.08.026)

This is a PDF file of an unedited manuscript that has been accepted for publication. As a service to our customers we are providing this early version of the manuscript. The manuscript will undergo copyediting, typesetting, and review of the resulting proof before it is published in its final form. Please note that during the production process errors may be discovered which could affect the content, and all legal disclaimers that apply to the journal pertain.



**Measuring mechanical parameters in glass fiber-reinforced composites:****Standard evaluation techniques enhanced by photogrammetry**

Isabel Koke <sup>a b \*</sup>, Wolfgang H. Müller <sup>b</sup>, Ferdinand Ferber <sup>a</sup>, Rolf Mahnken <sup>a</sup>, Herbert Funke <sup>c</sup>

<sup>a</sup> *Lehrstuhl für Technische Mechanik, Universität Paderborn, Pohlweg 47-49, 33098 Paderborn, Germany, isabel.koke@LTM.uni-paderborn.de, ferdinand.ferber@LTM.uni-paderborn.de, rolf.mahnken@LTM.uni-paderborn.de*

<sup>b</sup> *Lehrstuhl für Kontinuumsmechanik und Materialtheorie, Fakultät V, Institut für Mechanik, Technische Universität Berlin, 10587 Berlin, Germany, isabel.koke@tu-berlin.de, wolfgang.h.mueller@tu-berlin.de*

<sup>c</sup> *Fahrzeugkonstruktion, Fachbereich 5 / Maschinenbau, FH Dortmund, Sonnenstr. 96, 44139 Dortmund, Germany, herbert.funke@fh-dortmund.de*

**Abstract**

This paper demonstrates how the usual standard tests for characterization of mechanical stiffnesses of glass fiber-reinforced composites can be enhanced by means of photogrammetry. This method allows to reveal and study local imperfections and damage inherent to the production process of the material (e.g., weaving flaws) as well as during loading (e.g., fiber breakage). Moreover it is capable of quantifying the impact of these imperfections on design and construction in terms of (local) deformation or overall stiffness.

**Keywords:** A. Glass fibers; A. Fabrics/textiles; B. Mechanical properties, B. Stress/strain curves; C. Elastic properties

---

\* Corresponding Author

## 1. Introduction

For design purposes it is desirable to know as much as possible about the three-dimensional local deformation response in a structure made of fiber-reinforced materials. Accurate knowledge of their current anisotropic mechanical characteristics, in particular of the stiffness matrix, is required to reach this goal. Once the stiffnesses are known Finite Element (FE) studies in combination with suitable damage models can be used in order to assess and to predict the reliability of the whole structure. In order to quantify the stiffnesses key experiments, based on the concepts of laminate theory, have been conceived resulting in certain engineering standards, such as [1, 2].

...

## 2. Introduction

For design purposes it is desirable to know as much as possible about the three-dimensional local deformation response in a structure made of fiber-reinforced materials. Accurate knowledge of their current anisotropic mechanical characteristics, in particular of the stiffness matrix, is required to reach this goal. Once the stiffnesses are known Finite Element (FE) studies in combination with suitable damage models can be used in order to assess and to predict the reliability of the whole structure. In order to quantify the stiffnesses key experiments, based on the concepts of laminate theory, have been conceived resulting in certain engineering standards, such as [1, 2].

However, useful as these may be for a first mechanical assessment in terms of overall *initial* properties and, consequently, FE analysis of the *initial* stress-strain response, these standards are insufficient when the objective is a straightforward in-depth characterization of the quality of the production process leading to the laminate structure or of its residual properties during or after use.

Optical field measurement techniques are excellent tools that allow to retrieve this kind of information, the most prominent being classical photoelasticity [3], and more modern ones, such as Moiré or micro-Raman interferometry, e.g., [4, 5], speckle techniques [6] and, in particular, photogrammetry [7]. Depending on the material the structure is made of, all or at least some of these methods allow, in principle, to monitor the local 3D deformation. In combination with a suitable material law and the corresponding material parameters it then becomes possible to predict the local stresses, which together with the strains may eventually be entered in damage equations. However, these parameters are often unknown and, consequently, it becomes necessary to apply an “inverse method” by running an FE analysis with a suitable constitutive equation, assuming reasonable starting values for its material constants, predicting the

deformation pattern, comparing it with the experimental one, and reiterating this procedure until a “best fit” is achieved.

Clearly, to reach this objective in perfection is very ambitious. In this paper we will present a first attempt towards a solution of the full problem. More specifically, we will concentrate on a combination of experiments according to the standards described in [1, 2] together with photogrammetry to determine the in-plane elastic properties of a self-made glass fiber-reinforced laminate. This will allow us

- to discuss the non-linear stress-strain behavior of a virgin as well as a pre-conditioned laminate in terms of an average, a secant, and a second modulus;
- to determine the in-plane lateral contraction coefficient;
- to visualize and to quantify the onset and growth of local damage during loading of the structure due to ondulation, weaving flaws, warpage, and fiber breakage;
- to monitor the mechanical quality of a manually fabricated laminate and the corresponding production process.

Aside from this we will also briefly touch on the problems involved in the mechanical characterization of glass-fiber reinforced materials as indicated in the standard specifications. We will also outline the use and difficulties inherent to photogrammetry and put it in context with previous work in this field. The paper will end with a discussion of the results that were achieved so far, and how to improve them in the near future, e.g., by combining the deformation patterns obtained in photogrammetry with a finite element analysis in order to extract all current local elastic properties.

### **3. Specimen fabrication**

In order to determine the mechanical characteristics of handmade glass-fiber reinforced plastics (GRP) tensile test specimens were fabricated according to [1] as indicated in Fig. 1. More specifically, a glass fabric with a specific weight of 163 g/m<sup>2</sup> and finish

FRP 144 (Interglas 92110), in twill weave fashion was embedded in epoxy resin L1100 with a slow hardener EPH294 from *R&G Faserverbundwerkstoffe GmbH*, guaranteeing a processing time between 500 to 600 minutes [8]. Six or twelve of such fiber layers were required to produce specimens of 1 or 2 mm thickness, respectively. Some details of the manufacturing process are indicated in Fig. 2: The fabric is laminated on a base plate with a separation agent and a tearing fabric on top. The tearing fabric leads to a rough specimen surface which is very useful for firm attachment of tabs (see below). The laminated fibers obtain a label for identification. Moreover, strips of tearing fabric, plastic foil, cover and cushion are attached. After that the whole setup is sealed in a vacuum bag and left at room temperature for approximately 12 hours. Finally the testing laminate is tempered at approximately 70°C for 10 hours. The fiber volume fraction  $\varphi_F$  is determined with the following formula [9]:

$$\varphi_F = \frac{V_F}{V_L} = \frac{\rho_R \cdot m_F}{\rho_F \cdot m_R + \rho_R \cdot m_F} \quad (1)$$

where  $V_F$  denotes the volume of fibers in the laminate,  $V_L$  is total volume of the testing laminate,  $\rho_R$  and  $\rho_F$  are the (known) mass densities of the resin and of the fibers, respectively,  $m_F$  refers to the mass of the fibers in the laminate (the mass of the fibers per square meter is known and the area can easily be measured), and  $m_L$  is the mass of the laminate (to be obtained by weighing). Expected values of  $\varphi_F$  for hand laminates range between 35 % and 50 %; industrial laminates achieve 60 % or more.

The next step of preparation consists of attaching tabs (cf., Fig. 1) to the ends of the laminate. Tabs are required so that the load at the fixing grips of the tensile testing machine is properly transferred to the laminate giving rise to only very small stress concentrations and ensure that uniaxial stress conditions prevail. The last stage of

manufacturing consists of cutting out the tensile test specimens according to the German industry standard DIN EN ISO 2818: 1997, page 3, number 3.2. This is done with a diamond saw blade at a slow feeding speed (0.025 m/s) and a high number of revolutions (2950 1/min) assisted by water-cooling. Humidity absorption (determined according to DIN EN ISO 53495) was experimentally monitored showing that it is reversible by tempering the laminates for a short while.

#### 4. Setup and evaluation of tensile tests

In order to characterize the mechanical properties of the manufactured laminates tensile tests were carried out according to [1], as indicated in Fig. 3. The tests were displacement controlled, i.e., the force was recorded as a function of displacement  $u_y$  (measured with a mechanical extensometer) while increasing the load up to specimen failure. Displacements and forces were converted into axial engineering strain  $\varepsilon_y$  and uniaxial engineering stress  $\sigma_y$ . A typical result is shown in Fig. 4 (for the laminate GRP [0/90]<sub>12</sub> with a fiber volume fraction of 36%). Clearly the stress-strain relationship is *not* perfectly linear as it is commonly assumed in laminate theory. As we shall see shortly this is due to several effects, non-linearity of the resin, local imperfections of the material, imperfect alignment of the fibers, etc. Consequently the question arises how, on the basis of the available data, the linear-elastic stiffnesses of the material in question can rationally be determined. Two procedures were used for this purpose: In a *simplified approach* (shown in the left picture of Fig. 4) the stress-strain data was approximated by linear regression where the slope of the regression line served directly as a measure of Young's modulus. This is easily achieved. Note that the regression line does not quite lead through the origin of the stress-strain coordinate system. Moreover it is well known in experimental mechanics that this origin is always

hard to determine, which is due to slight fluctuations of the displacement control of the machine and to unavoidable (slight) initial misorientation of the specimen as well as (slight) deviation from proper uniaxial tensile loading conditions at the beginning of each test. This in turn renders it almost impossible to determine Young's modulus exactly as the initial slope of a stress-strain curve, even if the material is fully isotropic and without need for pre-conditioning (see below). It is for this reason that in more complex evaluation techniques the determination of the origin and follow-up re-adjustment of the stress-strain data points has become part of an iterative procedure for the determination of Young's modulus (see, e.g., [10]). However, in order to avoid mathematical intricacies we follow in the present paper a procedure known as the *bimodal approach* [11]: The stress-strain curve is divided into two regions (see Fig. 4, right, and Fig. 5) which can be distinguished by a bent, the so called "knee." Up to 0.1 % of strain the stress-strain data form almost a straight line the slope of which essentially coincides with that of a secant to the stress-strain curve. This slope, another measure of Young's modulus, is also known as the "secant modulus" (the DIN standards [1] and [12] recommend  $\epsilon = (0.05 \% , 0.25 \%)$  and  $\epsilon = (0.05 \% , 0.1 \%)$  to be used as the base points of the secant). In fact, the secant modulus represents the highest gradient (slope) and results at the beginning of the first loading of a virginal specimen. At ca. 0.4 % of strain the stress-strain curve of the virginal specimen flattens. The stress-strain data to the right of this knee are also fitted linearly and, consequently, result in a third measure of stiffness, the so-called "second modulus." The corresponding slope is clearly smaller than that of the secant modulus.

We conclude that the stress-strain behavior of a virginal test specimen is *not* strictly linear and cannot be described by a *single* stiffness. It is for this reason that we perform "cyclic" tensile tests by, first, applying a tensile load which steadily increases up to a

maximum value of 7.5 kN, followed by unloading to 1 kN and subsequent reloading to 7.5 kN, etc., until failure of the specimen. Fig. 5 presents the stress-strain curves after three such loading cycles. As previously discussed the stress-strain response during first load is non-linear and can be evaluated in the manner described above. However, the stress-strain curves of follow-up unloading and loading processes essentially coincide and, what is more, they are linear resulting in only one slope and, consequently, a single stiffness value. In other words after pre-conditioning the mechanical response of the laminate can sufficiently be described within the framework of linear, anisotropic elasticity, i.e., simple laminate theory. The pre-conditioning effect might eventually be explained micro-mechanically. It seems very likely that during first loading and subsequent unloading the fibers will start to align properly which, macroscopically speaking, would result in a reproducible stiffness value. Other explanations of the pre-conditioning phenomenon are that some kind of relaxation might take place between the fiber and the matrix, that the undulated fibers are stretched in loading direction, or that this effect results from the grips, i.e., the fixation of the specimen. Microsectioning of the virgin as well as of the pre-conditioned specimens should be able to confirm these suppositions. For now we conclude that unloading and subsequent reloading leads to a linear stress-strain response. The corresponding slope is in between the secant and the second modulus.

Clearly, there is a certain scatter involved in the stress strain data of virgin laminates of the same sort. This is demonstrated in Fig. 6 where five specimens of the GRP [0/90]<sub>6</sub> type with a fiber volume fraction of 38.5 % were tested leading to average secant and second moduli of 20 GPa and 15 GPa, respectively, with a standard deviation of roughly 500 MPa. Moreover, the photogrammetry experiments described below will show that there are also *local* fluctuations of the stiffness within each

specimen. This in turn explains the standard deviation observed for the *global* specimen stiffnesses which are characterized by the secant and second moduli as outlined above.

Fig. 7 allows to compare the stiffness obtained by linear regression (denoted as “approximation”), the secant and, finally, the second modulus for GRP [0/90]<sub>6</sub> with 38.5 and 37.2 vol. %. We conclude that the impact of the fiber volume fraction on stiffness seems insignificant at least within the accuracy of measurements and for the range of volume fractions considered. This is confirmed by the two Young’s moduli stemming from laminate theory which were calculated using the software *LamiCens* [13]. For the calculation several input parameters are required, such as the type of reinforcement fabrics or uni-/multidirectional inlays, the type of epoxy resin and the hardener. In addition the stacking sequence, the direction of the fibers and, of course, the fiber volume fraction need to be added.

Note that the average secant modulus from the test series essentially agrees with the *LamiCens* prediction according exceeding it by a maximum of 7 %. The stiffness values resulting from linear regression and the second modulus are smaller and close to each other.

## **5. Setup and evaluation of field optical measurements (photogrammetry)**

In the past field optical measurement techniques have frequently been used by the authors. In [5] Raman spectroscopy was used to reveal and quantify the local stress-strain distributions in particle reinforced ceramics. In [14-16] the mechanics of interface cracking was investigated by means of photoelasticity and other optical methods of experimental mechanics. In this paper photogrammetry will be used to visualize and quantify the full deformation fields in laminates subjected to uniaxial stress. More specifically, GOM’s commercial hardware/software package *Aramis* was

used. An introduction to the fundamentals as well as details of how and where this package can be used are compiled in [17,18]. By definition photogrammetry is a measurement technique where three-dimensional coordinates of points on an object are determined by using two photographic images taken at different positions [7]. To this end it is necessary to print a recognizable stochastic pattern onto the specimen's surface. As indicated in Fig. 8 a picture is taken by each camera during every step of the experiment, which can be both, load or displacement controlled (as it was in our case). A 3D displacement vector and (by differentiation) the corresponding strains on the specimen surface can then be obtained numerically in an automated fashion. It is worth mentioning that the Aramis-4M-system, which was used, consisted of two CCD cameras with a resolution of four mega pixel each. According to the manufacturer this will guarantee an accuracy of 0.01 % during strain measurements.

Fig. 9 shows the axial strain field  $\varepsilon_y$  of a GRP specimen  $[0/90]_6$  at various steps of *uniaxial* loading. Ideally, the strain field should be *homogeneous*. However, the color spots show that there are heterogeneities present in the specimen, which lead to local strain concentrations: A characteristic pattern in form of a diagonal structure appears when the stress is increased. The strain at the surface of the specimen obviously corresponds to the way the glass fabric is weaved (twill 2-2: one fiber crossing two others). The characteristic features of twill weaves are parallel diagonals or twill lines that are formed by the arrangement of interlacing points (where the warp and weft cross). The twill weave generates forces in the fabric that act along the twill lines. These forces can give rise to tension in the laminates which are strong enough to lead to bending when they have not been laid up uniformly [19].

Note that the first fibers cracked audibly at step 16. This was investigated closer by looking at the axial strain on the specimen surface along a virtual line (the so-called

“section line”): Fig. 10, left. At the beginning of the experiment the strain along the section line is nearly homogeneous. Then at step 16 some fibers break and the strain at the corresponding location jumps: Fig. 10, right, red curve.

This effect is examined closer in Fig. 11 which presents the development of the strain component  $\varepsilon_y$  for three different points on the specimen surface. “Stage point 2” corresponds to the location where the fiber cracking took place. And, indeed, for this point we observe a sudden jump, i.e., a strain discontinuity  $\varepsilon_y$  (i.e., crack opening) after a certain stress has been applied, whereas the strain in the other points increases monotonically.

The same procedures can now be applied to study the behavior of the lateral strain field  $\varepsilon_x$  of the GRP specimen: Fig. 12. By combining the strain results for the  $x$ - and  $y$ -direction another macroscopically relevant material parameter can be obtained: the lateral Poisson’s ratio (see Fig. 13). Specifically, we choose two section lines within the undamaged region of the specimen as shown in the strain carper plot on the right hand side of Fig. 13 and compute:

$$\nu_{xy} = \frac{|\varepsilon_x|}{\varepsilon_y} = \frac{0.044}{0.386} = 0.11. \quad (2)$$

This is very close to the prediction  $\nu = 0.1$  by *LamiCens*. Finally the slopes of the stress-strain curves corresponding to different points on the laminates, such as the ones shown in Fig.’s 10-13, can be used to calculate Young’s moduli characteristic of the overall stiffness behavior of the laminate in question. This has been done for a GRP  $[0/90]_6$  laminate using three such “virtual extensometers” resulting in the stiffness values of Table 1 (all values in MPa, nomenclature corresponding to Fig. 7).

## 6. Summary and outlook

In this paper it was shown how industry standards can be used for evaluation of stress-strain data resulting from uniaxial tensile tests to deliver stiffness coefficients of handmade glass-fiber reinforced laminates. It was shown that the stress-strain response of a virgin laminate is somewhat non-linear necessitating use of different stiffnesses, such as an average, a secant and a second Young's modulus. Moreover, it was demonstrated that pre-conditioning of a laminate by subjecting it to a sequence of loading and unloading states resulted in a linear stress-strain curve, which could be characterized by a single stiffness coefficient. The reason for this behavior is micromechanical, at least in part, stemming from realignment of the fibers as well as relaxation of the epoxy matrix.

Finally photogrammetry was used to determine several material characteristics in one experiment, namely Young's modulus and Poisson's ratio from field information regarding the displacements  $u_x$  and  $u_y$  or strains  $\varepsilon_x$  and  $\varepsilon_y$ , respectively.

Photogrammetry is also capable of assessing heterogeneities, i.e., the micromechanical behavior of composites, in particular the onset of fiber fracture, and inhomogeneities induced by the fabrication process.

Clearly, the vast amount of information hidden in the local displacement fields should be further analyzed. Several options exist, for example, a computer simulation of the tensile test could be performed, using FE in combination with suitable material laws, to predict the stress-strain fields during loading. This data could then be compared with the real stress-strain fields leading to an iterative procedure with the objective to extract optimum average or, if desired, optimized local material properties of GRPs. For this purpose we will build upon the "inverse method" techniques presented in [20], [21].

A detailed analysis of the material anisotropy, i.e., the determination of the different Young's moduli, Poisson's ratios, and shear moduli depending on the fiber orientation and weaving is left to future research.

### **Acknowledgments**

We thank *R&G Faserverbundwerkstoffe GmbH*, Waldenbuch, for supporting the experimental work. One of the authors (I.K.) would also like to thank for financial support of this work as part of the BMBF project *Nemesis – Virtual Engineering Labs*.

### **References**

- [1] DIN EN ISO 527: Bestimmung der Zugeigenschaften. Teil 1: Allgemeine Grundlagen; Teil 4: Prüfbedingungen für isotrope und anisotrope faserverstärkte Kunststoffverbundwerkstoffe.
- [2] ASTM. 1989. Standard test method for tensile properties of fiber reinforced composites. ASTM Standards; Vol. 15.03: 117-121.
- [3] Föppl L, Mönch E. Praktische Spannungsoptik. Springer Verlag, Berlin, 1950.
- [4] DeWolf I, Maes HE, Jones SK. Stress measurements in silicon devices through Raman spectroscopy: Bridging the gap between theory and experiment. *Journal of Applied Physics* 79 (9): 7148-7156, 1996.
- [5] Pezzotti G, Müller WH. Micromechanics of fracture in a ceramic/metal composite studied by in-situ fluorescence spectroscopy I: Foundations and stress analysis. *Cont. Mech. Thermodyn.* 2002; 14(1): 113-126.
- [6] Handbuch für experimentelle Spannungsanalyse. Editor C. Rohrbach, Speckle Verfahren, pp. 419, VDI Verlag, 1989.

- [7] Handbuch für experimentelle Spannungsanalyse. Editor C. Rohrbach, Photogrammetrie, pp. 419, VDI Verlag, 1989.
- [8] R&G Catalogue. Waldenbuch, 1<sup>st</sup> edition, 2006.
- [9] Carlsson LA, Pipes BR. Experimental Characterization of Advanced Composite Materials. Prentice-Hall, Inc., Englewood Cliffs, New Jersey, United States of America, 1987.
- [10] Andersson C, Liu L, Liu J. Characterization of Mechanical Properties of Eutectic Sn-Co-Cu Lead Free Alloy. 2006 Electronics Systemintegration Technology Conference, Dresden, Germany, 152-160.
- [11] Faserverbundwerkstoffe Band 3. Herausgeber J. Hansen, Springer Verlag Berlin, 1986, pp. 468.
- [12] DIN EN 2747: Glasfaserverstärkte Kunststoffe. Zugversuch.
- [13] Funke H. LamiCens. Software, R&G GmbH, Version 0.98, Dec. 2005.
- [14] Ferber F. Bruchmechanische Analyse der Entstehung und Ausbreitung von Matrix- und Grenzflächenrissen in thermisch belasteten Faserverbundwerkstoffmodellen. Ph.D. Thesis, Universität Paderborn, 1986.
- [15] Ferber F. Numerische und experimentelle Untersuchungen rissbehafteter Strukturen. Berichte aus der Mikromechanik, habilitation thesis, Shaker Verlag, Aachen, 2001.
- [16] Ferber F, Herrmann KP, Linnenbrock K. Elementary failure analysis of composite models by using optical methods of stress analysis and modern digital image systems. In: ESDA 1996, (Eds. A. Large and M. Raous) ASME, New York, Vol. 4: 55-68, 1996.
- [17] Aramis v5.4, User Manual. GOM mbH 2005.

- [18] Galanulis K. Optical measuring technologies in sheet metal processing. Proceedings of SheMet 2005, Advanced Materials Research Vols. 6-8 (May 2005): 19-34, TransTechPublications.
- [19] R&G Handbuch. Waldenbuch, Edition 8, 2006.
- [20] Nguyen S, Herrmann KP, Müller WH, Albrecht H-J. Parameter identification of SMT solder materials using the small punch test. ZAMM 2001; 81 S4: S843-S844.
- [21] Albrecht H-J, Hannach T, Häse A, Juritza A, Müller K, Müller WH. Nanoindentation: A suitable tool to determine local mechanical properties in microelectronic packages and materials? Archive of Applied Mechanics 2005; 74 (11-12): 728-738.

### Figure captions

Fig. 1. Dimensions of tensile test specimen

Fig. 2. Production scheme for the manufacturing of testing laminates

Fig. 3. Tensile test setup

Fig. 4. Evaluation of uniaxial stress-strain data

Fig. 5. Stress strain curve of a cyclic tensile test using GRP  $[0/90]_{12}$ , fiber volume fraction 36% (see text)

Fig. 6. Tensile test series for GRP  $[0/90]_6$ , fiber volume fraction 38.5 %

Fig. 7. Comparison of Young's moduli for GRP  $[0/90]_6$  with 38.5 and 37.2 vol. % of fibers determined with different methods (see text)

Fig. 8. The principle of photogrammetry demonstrated for a tensile test

Fig. 9. Optical representation of the development of the strain field  $\varepsilon_y$  in a GRP  $[0/90]_6$  laminate subjected to uniaxial loading; first line: loading step; second and third line: current load and stress

Fig. 10. Strain  $\varepsilon_y$  along a section line and identification of first fiber cracks

Fig. 11. Development of  $\varepsilon_y$  at three positions

Fig. 12. Sampling local  $\varepsilon_x$  data along a section line, at three positions and field information in an overlay at time of fiber cracking

Fig. 13. Stress strain curves for  $\varepsilon_x$  and  $\varepsilon_y$  determined by a “virtual extensometer” shown on the right hand sight

#### Tables

Table 1: Young’s moduli predicted from virtual extensometry (for nomenclature see Section 3)

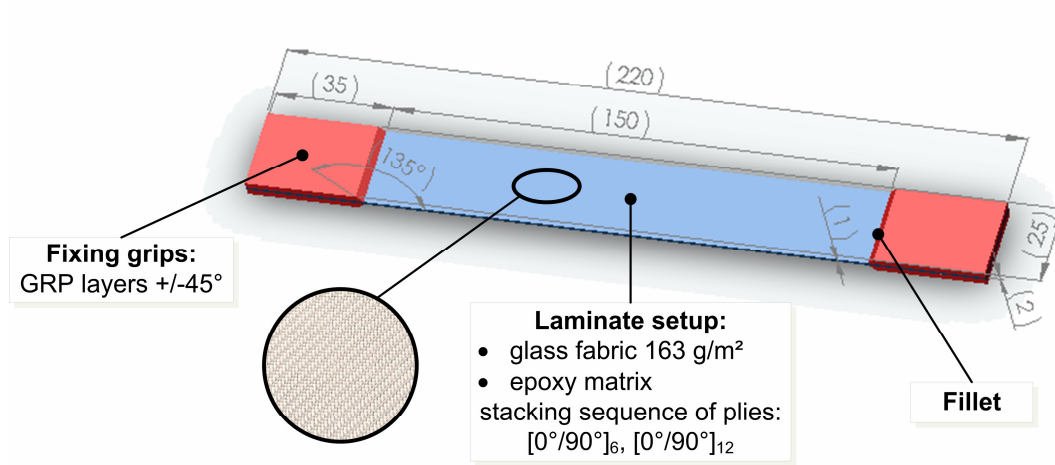


Fig. 1. Dimensions of tensile test specimen

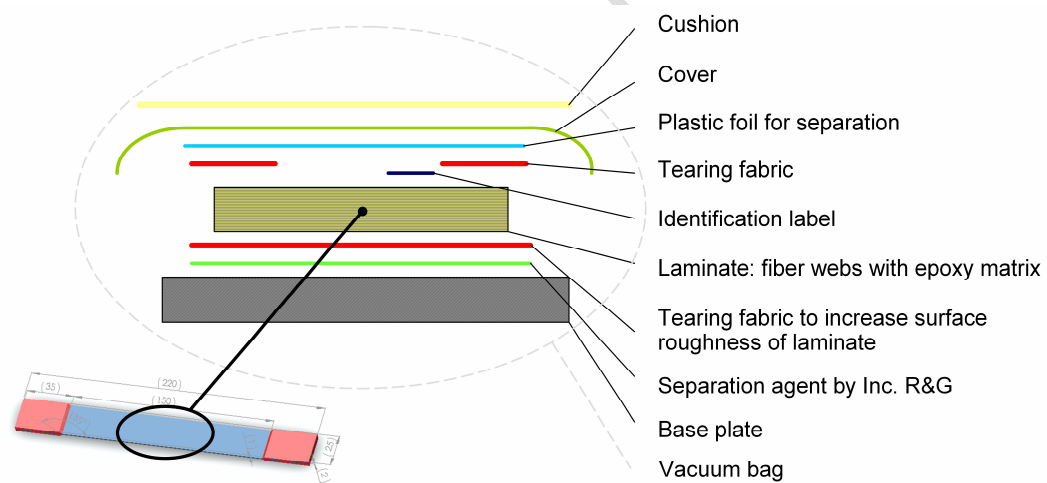


Fig. 2. Production scheme for the manufacturing of testing laminates

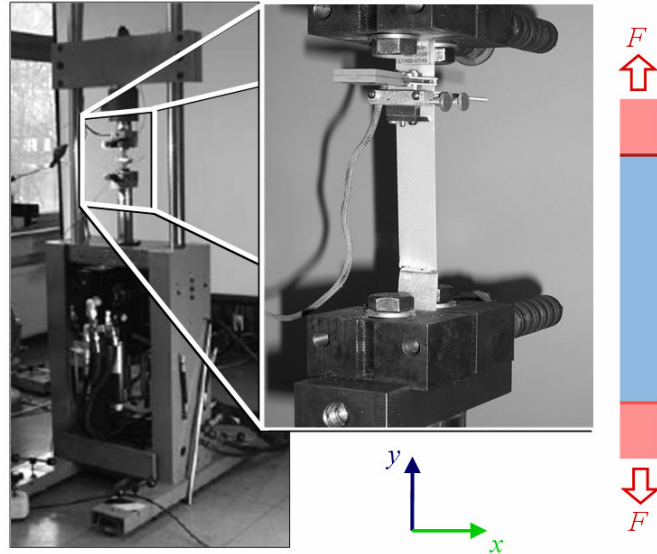


Fig. 3. Tensile test setup

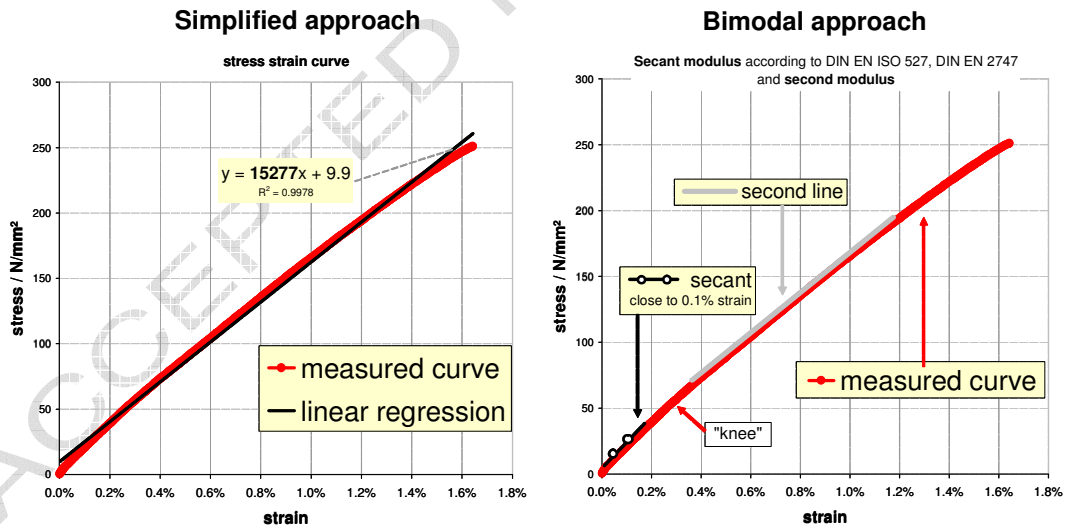


Fig. 4. Evaluation of uniaxial stress-strain data

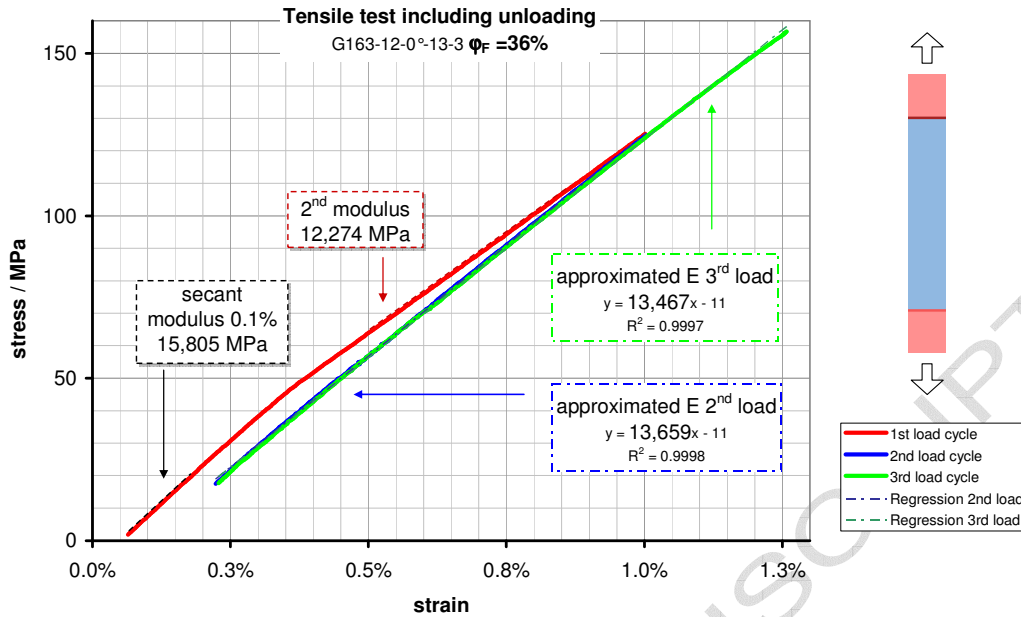


Fig. 5. Stress strain curve of a cyclic tensile test using GRP [0/90]<sub>12</sub>, fiber volume fraction 36% (see text)

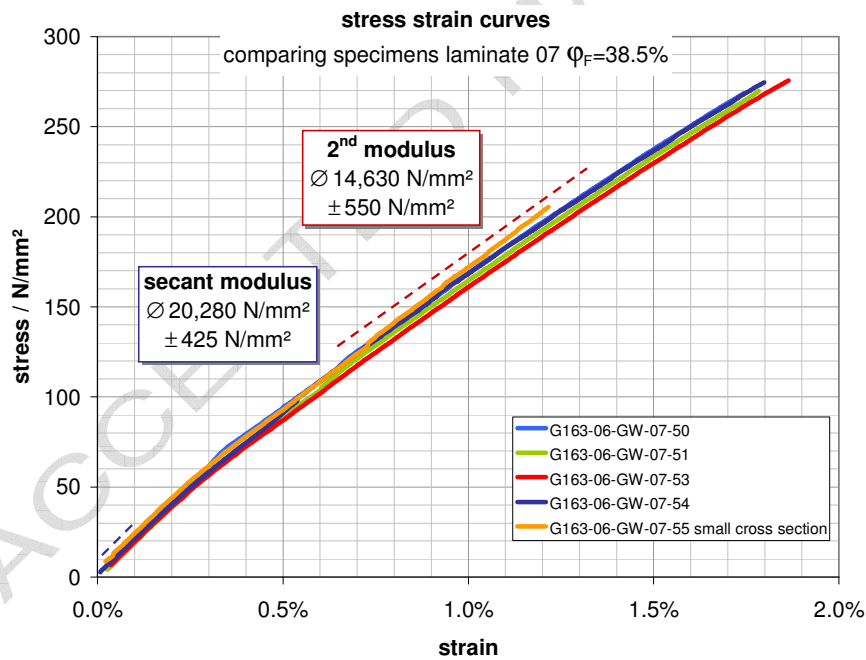


Fig. 6. Tensile test series for GRP [0/90]<sub>6</sub>, fiber volume fraction 38.5 %

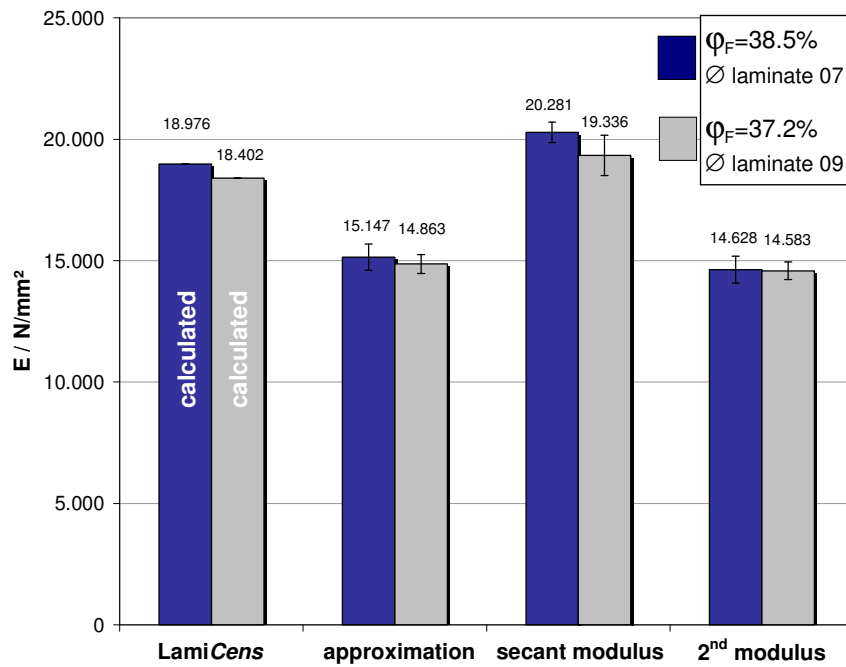


Fig. 7. Comparison of Young's moduli for GRP  $[0/90]_6$  with 38.5 and 37.2 vol. % of fibers determined with different methods (see text)

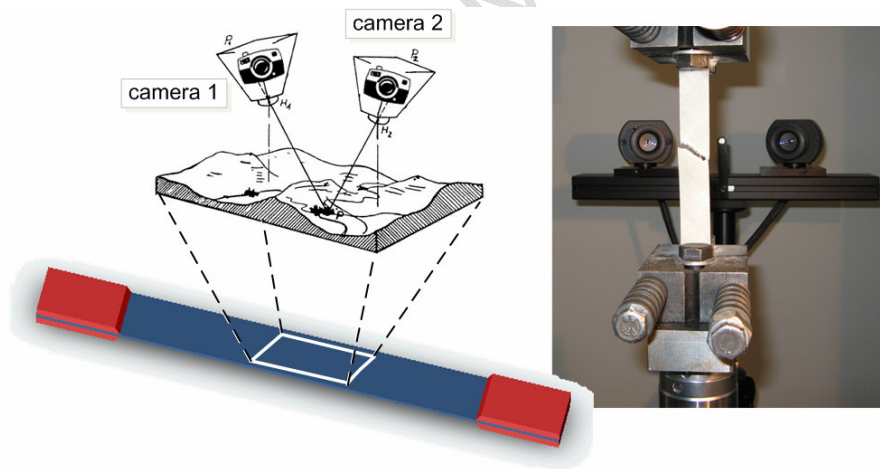


Fig. 8. The principle of photogrammetry demonstrated for a tensile test

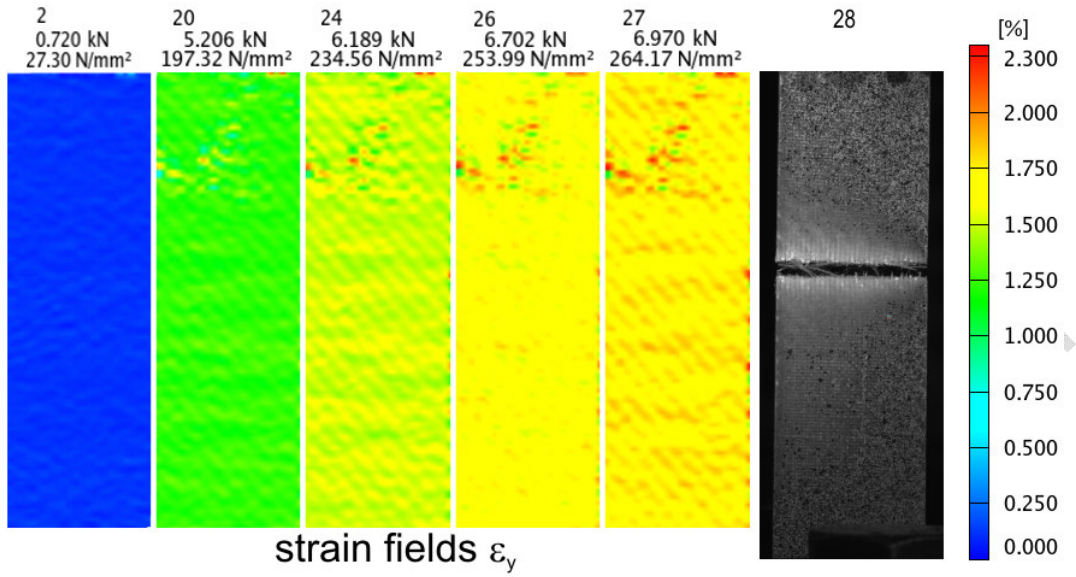


Fig. 9. Optical representation of the development of the strain field  $\varepsilon_y$  in a GRP  $[0/90]_6$  laminate subjected to uniaxial loading; first line: loading steps; second and third line: current load and stress

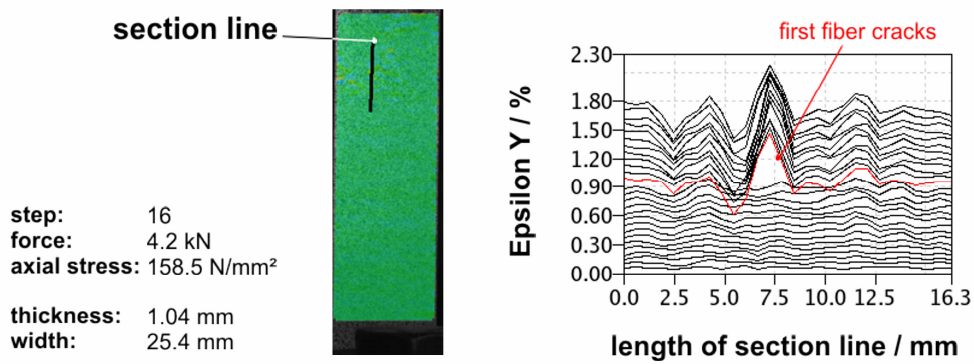


Fig. 10. Strain  $\varepsilon_y$  along a section line and identification of first fiber cracks

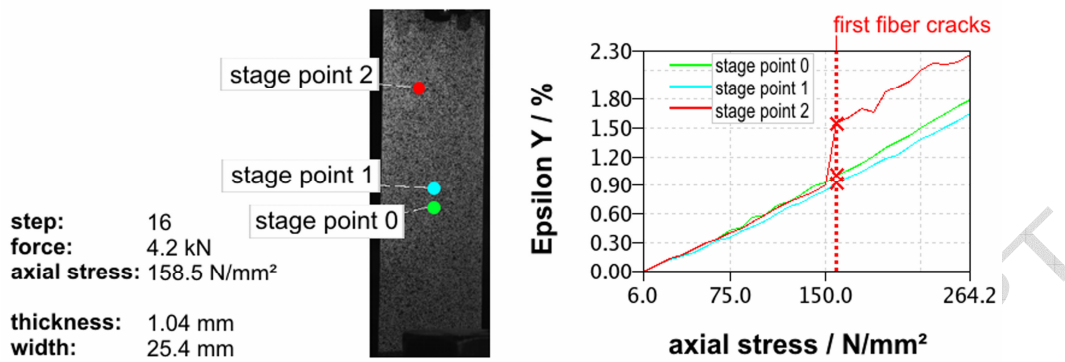


Fig. 11. Development of  $\varepsilon_y$  at three positions

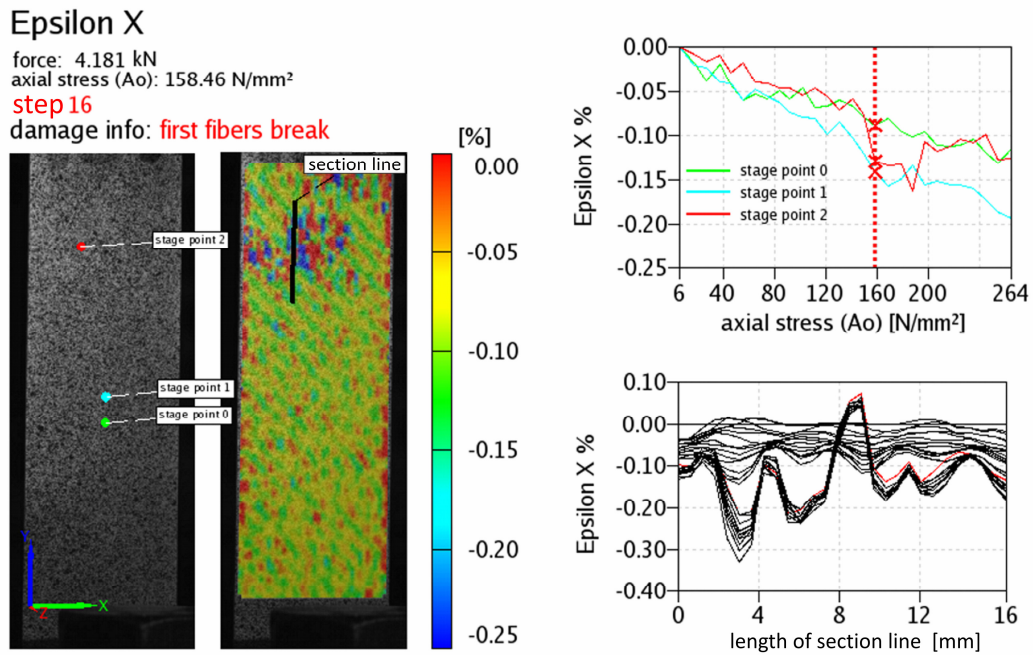


Fig. 12. Sampling local  $\varepsilon_x$  data along a section line, at three positions and field information in an overlay at time of fiber cracking

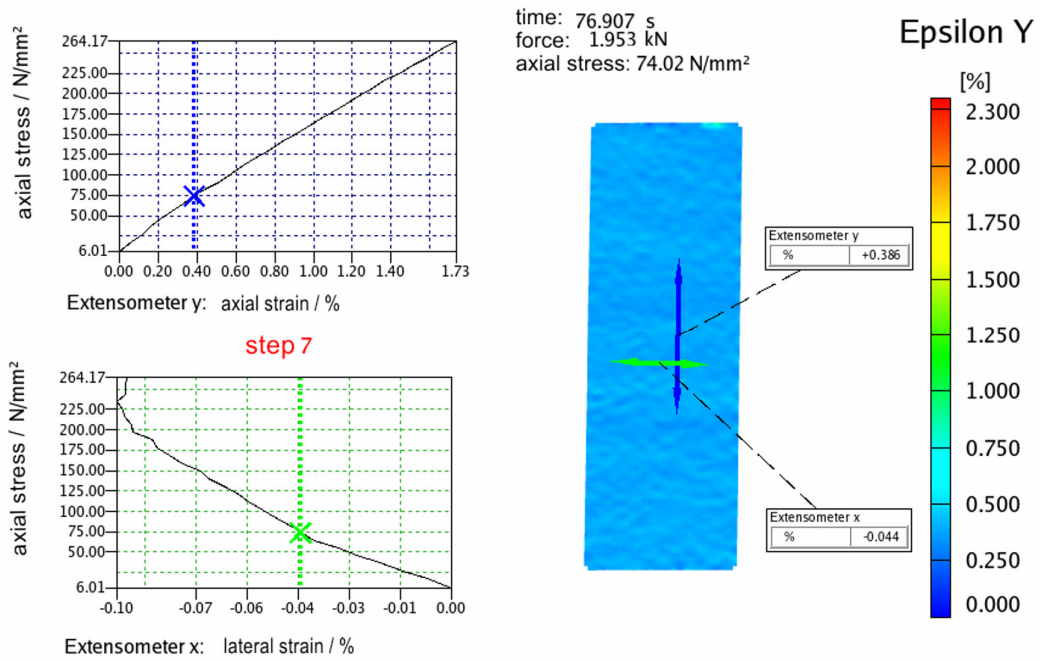


Fig. 13. Stress strain curves for  $\varepsilon_x$  and  $\varepsilon_y$  determined by a “virtual extensometer” shown on the right hand side

**Tables**

Table 1: Young's moduli predicted from virtual extensometry (for nomenclature see Section 3)

approximation	secant modulus $\epsilon = (0.05 \% , 0.15 \%)$	secant modulus $\epsilon = (0.05 \% , 0.15 \%)$	second modulus
$14780 \pm 81$	$18305 \pm 139$	$18636 \pm 116$	$14078 \pm 66$